JOURNAL OF APPLIED PHYSICS VOLUME 94, NUMBER 4 15 AUGUST 2003

Current limiting mechanisms in indium-tin-oxide/poly3-hexylthiophene/aluminum thin film devices

Z. Chiguvare, J. Parisi, and V. Dyakonov[a)]
Department of Energy and Semiconductor Research, University of Oldenburg, D-26111 Oldenburg, Germany

(Received 10 March 2003; accepted 10 May 2003)

We studied the temperature dependent current-voltage characteristics of regioregular poly (3-hexylthiophene 2.5-diyl) (P3HT) thin films sandwiched between indium tin oxide (ITO) and aluminum (Al) electrodes (ITO/P3HT/Al devices), with the aim of determining the current limiting mechanism(s) in these devices, and the temperature and/or applied electric field range(s) in which these mechanisms are valid. The current-voltage characteristics of the ITO/P3HT/Al devices showed that current flow across the device is limited by hole injection at the Al/P3HT interfaces at temperatures below 240 K, when the device is biased with high potential on Al. Above this temperature, the bulk transport properties control the characteristics. For the reverse bias, the ITO/P3HT contact does not limit the current; instead it is controlled by a space charge that accumulates due to the low charge carrier mobility in the polymer. An expression that provides a criterion to determine the validity of applying either the Richardson–Schottky thermionic emission model or the Fowler–Nordheim field emission model was deduced. It can be employed to determine the electrical field at which the transition from charge injection by thermionic emission to that by field emission for a given temperature and interface potential barrier height takes place. Our experimental data fit to the deduced expression. Theoretical limits of the model are also discussed. By considering the regions of the current-voltage curves where field emission or thermionic emission was applicable, the interface potential barriers were estimated, respectively. Hence, conclusions on whether the current-voltage behavior of the devices was contact limited or bulk limited could be drawn. © *2003 American Institute of Physics.* [DOI: 10.1063/1.1588358]

I. INTRODUCTION

A. Motivation

The ease of processing of conjugated polymers and the ability to form large area thin films on virtually any, including mechanically flexible, substrates makes these materials very attractive for use as active components for efficient light emitting diodes (LEDs), solar cells, and other solid state electronic devices like Schottky diodes and field effect transistors (FETs). Transport properties of electrically conducting polymers are of great academic and practical interest.[1,2] However, in spite of significant advances in the understanding of the qualitative behavior of organic light emitting diodes, a fully quantitative description of charge injection at the electrodes, charge transport in the bulk, and electron-hole recombination has yet to emerge.[3,4] The rapidly expanding field of organic electronic devices and the wide application of organic films in electrophotography have stimulated a lot of attention and research on fundamental questions concerning metal/organic semiconductor interfaces.[5]

Effective charge injection and transport in thin films of conjugated polymers play a key role in high performance polymer LEDs and FETs. Thereby, research has focussed on the charge transport processes that limit current across the sample, and hence, the number of electrons and holes available for radiative recombination.[6] Most of the principles applicable to LEDs are also applicable to photovoltaic solar cells. The functioning of organic LEDs is based on the injection of both holes and electrons from the electrical contacts, their migration into the bulk followed by recombination, and the radiative decay of the excited state produced in the course of mutual annihilation of a pair of charge carriers.[7,8] The aim is to inject a balanced amount of electrons into the conduction band and holes into the valence band, thus creating conditions favorable for recombination, leading to the emission of visible radiation (light). In solar cells, the aim is to absorb as much light as possible, creating charge carriers, i.e., holes in the valence band and electrons in the conduction band, which must be separated, transported in the bulk, and then effectively collected through the electrodes to the outer circuit.[9,10] A high performance FET must have a high current output, a high mobility of charge carriers through the channel, and a high on/off ratio.[11,12] To improve the performance of polymer LEDs, FETs, and solar cells, it is vital to understand what mechanisms control the current-voltage characteristics of a given device structure. In any such applications the manner in which electrical contact is made to the polymer is of crucial importance.

We studied temperature dependent current-voltage (J-V) characteristics of regioregular poly (3-hexylthiophene 2.5-diyl) (P3HT) thin films sandwiched between indium tin oxide (ITO) and aluminum (Al) electrodes (ITO/P3HT/Al devices), with the aim of determining the current limiting

[a)]Author to whom all correspondence should be addressed; electronic mail: dyakonov@uni-oldenburg.de

Downloaded 05 Aug 2003 to 134.106.114.81. Redistribution subject to AIP license or copyright, see http://ojps.aip.org/japo/japcr.jsp

mechanism(s) in these devices, and the electric field and temperature range(s) in which these mechanisms are valid. A relationship between the applied field, the temperature, and the rigid Schottky barrier was established, which can be used to determine the threshold conditions for transition from field emission to thermionic emission dominated current-voltage behavior. This expression seemed to be applicable to, and to agree well with, the measured data from our experiments. The limits of applicability of this relationship were also explained theoretically. By considering the regions of the J-V curves where field emission or thermionic emission was applicable, the interface potential barriers were estimated, respectively. Hence, conclusions on whether the current-voltage behavior of the devices was contact limited or bulk limited, could be drawn.

B. Modeling of current in metal/polymer/metal structures

The current-voltage characteristics of metal/polymer/metal devices are controlled by two basic processes: (a) injection of charge carriers from the electrodes into the polymer and vice versa and (b) transport of charge in the bulk of the film. Steady state current is determined by the less effective mechanism, since this is the one that limits net charge flow depending on the specific experimental situation (the externally applied electric field, the height of the injection barrier, i.e., the difference between the electrode work function and the corresponding transport levels of the polymer, and the temperature, etc.). The current is then either injection limited or bulk transport limited.

To be injected into the polymer, the charge carriers must overcome the potential barrier at the metal/polymer interface. As is the case for small barriers or at high temperatures, a large number of charge carriers will have energies large enough to cross the interface barrier in the classical way—denoted thermionic emission.[13] But when the temperature decreases or when the potential barrier height presents a large value, a reduced number of charge carriers has energies larger than the potential barrier height, and the thermionic emission becomes insignificant. The injection then can only occur via quantum mechanical tunneling through the potential barrier. The charge carriers tunnel from the metal to the empty states at the lowest unoccupied molecular orbital (LUMO) or at the highest occupied molecular orbital (HOMO) level in the polymer. Alternatively, if the polymer layer contains a high concentration of impurities, the tunneling may occur from the metal to empty localized states in the polymer layer, constituting a hopping-type process.[14] It is the smallest barrier at each interface which always dominates the injection.[15]

An ohmic contact is defined as an infinite reservoir of charge that is able to sustain a steady state space charge limited current (SCLC) in a device. With ohmic contacts, the current-voltage relation is often linear at low bias up to a certain value since the electrical field due to the injected carriers is negligible compared to that due to the applied bias. The slope of a log–log plot between current I (or current density J), and voltage V at low voltages is then equal to 1, and the behavior is described by Ohm's law, Eq. (1):[16]

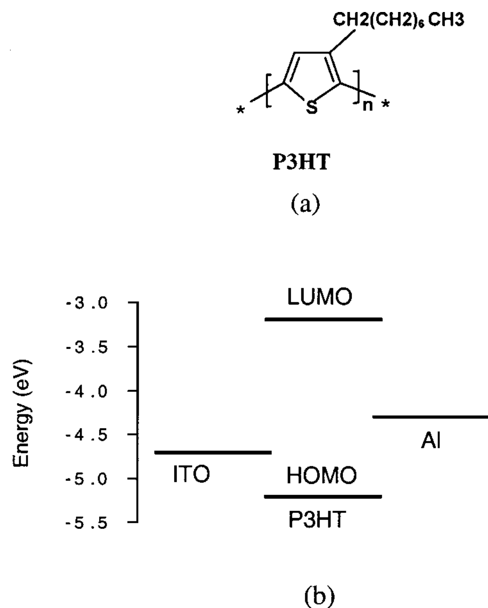

FIG. 1. (a) Chemical formula of poly(3-hexylthiophene 2.5-diyl) (P3HT) and (b) energy level diagram of the devices studied (under nonequilibrium conditions).

$$J_{\mathrm{ohm}}=qn\mu\frac{V}{d}, \tag{1}$$

where q is the electronic charge, n the charge carrier density, μ the carrier mobility, V the applied voltage, and d the thickness of the sample. This condition breaks down at the space charge limit when the injected carrier density becomes so large that the field due to the carriers themselves dominates over that of the applied bias and then becomes space charge limited. SCLC occurs when the transit time of any excess injected carrier is less than the bulk dielectric relaxation time. Under these circumstances, the trap free space charge limited current (TFSCLC) takes the simple form of Child's law [see Eq. (2)]. This behavior is characterized by a strict quadratic dependence of current on voltage (slope 2 in a $\log J$-$\log V$ plot). (Note that this does not necessarily imply the absence of traps in the material, but rather that they are all filled).[17]

$$J_{\mathrm{TFSCL}}=\frac{9}{8}\varepsilon_o\varepsilon_r\mu\frac{V^2}{d^3}. \tag{2}$$

Here, ε_r and ε_o are relative permittivity and permittivity of free space, respectively. Space charge limited currents in a device can occur if at least one contact[6] is able to inject locally higher carrier densities than the material has in thermal equilibrium without carrier injection. An emission limited contact is one that falls short of an ohmic contact's ability to supply charge. The emission limitation can range from totally blocking to finite injecting.[18]

II. MATERIALS AND METHODS

The formula of P3HT and a comparative energy level diagram of the studied device (under nonequilibrium conditions) are shown in Fig. 1. The HOMO of P3HT has been estimated to range between 5.1 and 5.2 eV, from an SCLC

Downloaded 05 Aug 2003 to 134.106.114.81. Redistribution subject to AIP license or copyright, see http://ojps.aip.org/japo/japcr.jsp

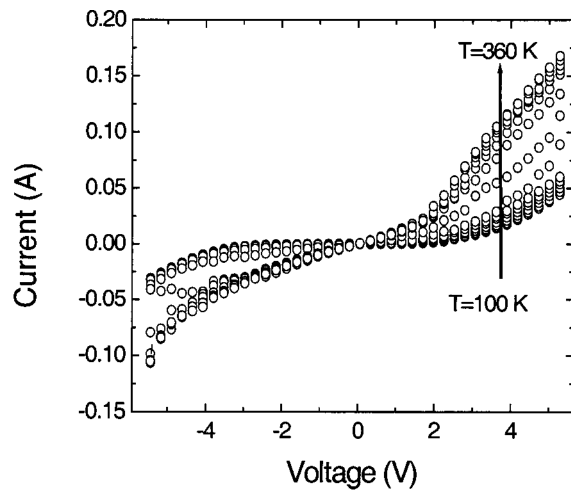

FIG. 2. An overview of current-voltage curves for $d=20$ nm thick ITO/P3HT/Al devices within the 100 to 360 K temperature range.

analysis of hole only thin film devices,[19] cyclic voltametry,[20] and photoelectron spectroscopy.[21] The energy gap estimated from absorption spectroscopy is about 2.1 eV, therefore the LUMO is about 3.0 eV. The work functions of ITO and Al are about 4.7 and 4.3 eV, respectively.

The high work function electrode was patterned by etching commercial ITO coated glass substrates in acid. The substrates were cleaned in deionized water, acetone, toluene, and isopropanol, respectively, in a hot ultrasonic bath. A chloroform-toluene based polymer solution (P3HT, 5 mg/ml) was then spin-coated in the nitrogen atmosphere of a glove box, O_2-2 ppm and H_2O-0,01 ppm. The metal top electrode (Al) was deposited by thermal evaporation in high vacuum, better than 5×10^{-7} mbar, at a slow rate of between 0.05 and 0.1 nm/s.

All devices were stored in nitrogen atmosphere prior to measurement. Dark, temperature dependent, current-voltage characteristics were obtained by utilizing a dc current-voltage Source/Monitor Unit (Advantest TR 6143), as a voltage source and current monitor, with the device placed in a liquid-nitrogen-cooled cryostat at high vacuum of better than 10^{-5} mbar in all cases. The temperature range studied was from 100 to 360 K, and the temperature was allowed to stabilize for 3 min within $+/-0.1$ K before measurement was initiated. The thickness of the devices was then obtained by scrapping off part of the thin polymer film, and using an atomic force microscope (Burleigh Vista -100 Scanning Probe Microscope), in the non-contact mode, to scan the formed step.

III. RESULTS AND DISCUSSION

A. Current-Voltage characteristics

An overview of the current (I) versus voltage (V) characteristics of ITO/P3HT/Al devices, for temperatures ranging from 100 to 360 K, is shown on a linear scale in Fig. 2. The asymmetrical nature of the curves is attributed to the difference in the work functions of the electrodes, implying different barriers at each electrode/polymer interface.

Figure 3 shows double-logarithmic J-V plots for different temperatures, ranging from 100 up to 360 K in 20 K steps. Figure 3(a) corresponds to hole injection into the HOMO of P3HT through Al (+ is on Al) and electron injection into the LUMO through ITO (− on ITO). It can be observed that the curves have a slope equal to about 1 at low voltages, suggesting compliance with Ohm's law. It is interesting to note that the slope then tends to about 4, and each curve approaches this slope at a higher voltage, the higher the temperature. Since the slope is greater than 2, it might indicate the existence of traps within the bulk of the semiconductor.[16] The power dependence of current on voltage will be steeper than the quadratic one, if the distributed deep traps will influence the charge transport within the semiconductor bulk.

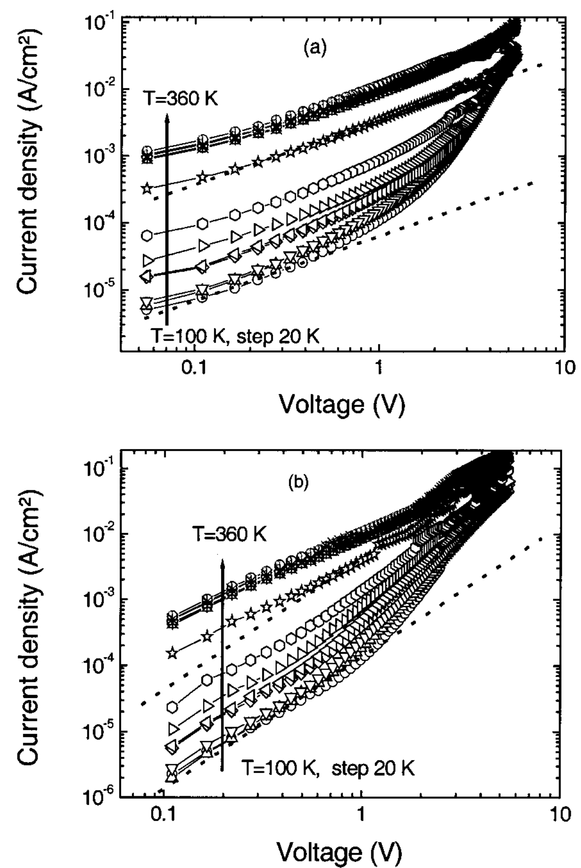

FIG. 3. J-V curves in log-log scale for (a) hole injection through the Al/P3HT interface (dotted lines correspond to slope (1) and (b) hole injection through the ITO/P3HT interface (dotted lines correspond to slope (2).

The limitation of the current by the contact with a relatively high barrier (such as the hole injection through Al/P3HT) is more pronounced at low temperatures. At such temperatures, thermally generated carriers are very few, and at low voltages the injected charge density is small so that the overall behavior is ohmic. As the voltage is increased, the number of injected carriers increases, so that space charge accumulates, tending to limit the current. The number of thermally generated carriers increases with temperature, hence, the current increases with temperature, conforming to semiconductor behavior. Therefore, an even higher voltage has to be applied before the injected charge and the thermally generated charge can become comparable. The super linear-

Downloaded 05 Aug 2003 to 134.106.114.81. Redistribution subject to AIP license or copyright, see http://ojps.aip.org/japo/japcr.jsp

ity is, therefore, expected at a higher voltage, when the temperature increases. Superlinear behavior [see Fig. 3(a)] suggests that the injected charge overwhelms the transport capabilities of the polymer, hence giving rise to the accumulation of positive charge near the Al hole injecting electrode. The bulk properties start to control the curent-voltage characteristics. When all the curves reach the constant slope line, the *J-V* curves depend more strongly on the voltage applied rather than temperature.

Figure 3(b) corresponds to electron injection into the LUMO of P3HT through the Al electrode, and hole injection into the HOMO through the ITO electrode. Below 2 V, the slope of the curves measured at low temperatures is approximately 2 (TFSCLC behavior). The bulk controls the current. At higher temperatures, the slope found is between 1 and 2. This means that the thermally generated carrier density exceeds that of the injected charge. The changes in slope with applied voltage seen in Figs. 3(a) and 3(b) are different due to the different hole injection barrier heights.

B. Thermionic emission

At low electrical fields when the slope of ln(*J*) versus ln(*V*) is about 1, the region is considered as being ohmic. Above the ohmic region, the current-voltage characteristics may be fitted to the Richardson–Schottky (RS) emission model. The essential assumption of the RS model of thermionic emission is that an electron from the metal can be injected into the polymer, once it has acquired a thermal energy sufficient to cross the potential maximum that results from the superposition of the external and the image charge potential. This model usually is valid at lower fields and higher temperatures. At higher fields, the metal work function for thermionic emission is reduced, thus lowering the Schottky barrier height (image force lowering). The Schottky equation, taking into account image force lowering, may be written as[22,23]

$$J=A^*T^2\exp\left(-\frac{\phi_B}{k_BT}\right)\exp\left[\left(\frac{q^3V}{4\pi\varepsilon_0\varepsilon_r d}\right)^{1/2}/k_BT\right], \qquad (3)$$

where ϕ_B, d, ε_0, and ε_r are the interface potential barrier height, film thickness, vacuum permittivity, and optical dielectric constant, respectively. k_B is Boltzmann's constant, q the elementary electronic charge, T the absolute temperature, and the applied voltage V is positive for forward bias and negative for reverse bias. A^* is the Richardson–Schottky constant $(A^*=4\pi qm^*k_B^2/h^3=120\ \mathrm{A/cm^2\,K})$, for free electrons, where the effective carrier mass m^* equals that of the free electron, otherwise it depends on the anisotropy of the material;[24] h is Planck's constant.

Equation (3) may be rewritten as

$$\ln\left(\frac{J}{T^2}\right)=\ln(A^*)+\left[\left(-\phi_B+\sqrt{\frac{q^3V}{4\pi\varepsilon_0\varepsilon_r d}}\right)\frac{1}{k_B}\right]\frac{1}{T}. \qquad (4)$$

According to Eq. (4), plots of $\ln(J/T^2)$ versus $1000/T$ are straight lines, since all the other parameters are constant, at a given voltage V. The expression in the square brackets of Eq. (4) represents the slope of $\ln(J/T^2)$ versus $1000/T$ and is called activation energy. The effective barrier height between the electrode and the film may be calculated from the slope, thus,

$$\phi_B=\left(-k_B\times slope+\sqrt{\frac{q^3V}{4\pi\varepsilon_0\varepsilon_r d}}\right). \qquad (5)$$

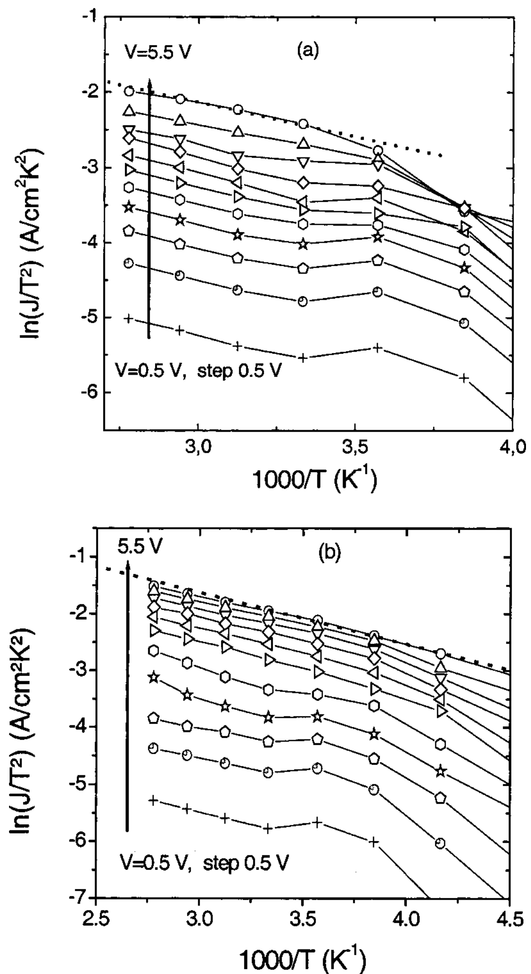

FIG. 4. $\ln(J/T^2)$ vs $1000/T$ plot for (a) hole injection through the Al/P3HT interface and (b) hole injection through the ITO/P3HT interface. Dotted lines are guides for the eye.

Our experimental data fits well with the RS emission model at high temperatures. As can be noted from Fig. 4, the slopes of $\ln(J/T^2)$ versus $1000/T$ at different voltages tend to straight lines at high temperatures. This is particularly clear in the case of hole injection through ITO, Fig. 4(b), where the straight lines are observed from about 250 K $(1000/T=4)$ upwards. In the case of Fig. 4(a), i.e., hole injection through Al, the straight line behavior seems to be evident above 300 K, but there are too few experimental points to make a reasonable fit. However, the fact that thermionic emission dominated behavior is observed at higher temperatures indicates that a higher hole injection barrier exists at the Al/P3HT interface, since more thermal energy is required before the charge carriers will be able to overcome it. This confirms the difficulty of injection through this barrier as compared to the ITO/P3HT interface as has been observed and mentioned in Sec. III A. The employment of Eq. (5) to

Downloaded 05 Aug 2003 to 134.106.114.81. Redistribution subject to AIP license or copyright, see http://ojps.aip.org/japo/japcr.jsp

the fitted straight lines yielded a hole injection barrier equal to 0.44 eV for the ITO/P3HT interface. A larger barrier is expected for hole injection through the Al/P3HT interface.

C. Field emission

The Fowler–Nordheim (FN) model for tunneling injection (field emission) ignores image charge effects and invokes tunneling of electrons from the metal through a triangular barrier into unbound continuum states. It predicts that when field emission dominates, the J-V characteristics are described by

$$J=AF^2\exp\left(-\frac{8\pi\sqrt{2m^*}\phi_B^{3/2}}{3hqF}\right), \tag{6}$$

where m^* is the effective charge carrier mass, F the applied electric field, and A [in A/V^2] a rate coefficient that contains a tunneling prefactor and the rate of current back-flow.[25] It can be deduced from the treatment by Kao and Huang[22] that A is given by

$$A=\frac{q^3}{8\pi h\phi_B}. \tag{7}$$

Equation (6) can also be written as

$$J=AF^2\exp\left(\frac{-\kappa}{F}\right), \tag{8}$$

where

$$\kappa=\frac{8\pi\sqrt{2m^*}\phi_B^{3/2}}{3qh}=\text{constant}. \tag{9}$$

If the value of κ is known, then the barrier height between the electrode and the film may be estimated from Eq. (9) as

$$\phi_B=\left[\frac{3\kappa qh}{8\pi\sqrt{2m^*}}\right]^{2/3}. \tag{10}$$

Equation (6) may be rewritten thus

$$\ln\left(\frac{J}{F^2}\right)=\ln A-\kappa\left(\frac{1}{F}\right). \tag{11}$$

This is a straight line equation of $\ln(J/F^2)$ versus $(1/F)$ with a slope equal to $-\kappa$, and the plot is referred to as the FN plot. The value of κ may, thus, be determined from FN plots. Figure 5 shows typical FN plots of ITO/P3HT/Al devices for temperatures ranging between 100 and 220 K for positive (a) and negative (b) bias on Al, respectively.

At high applied fields, the FN curves for our devices can be fitted to straight lines. From the slope of the straight part of FN plots, the interface potential barrier height can be computed by using Eq. (10). In Fig. 5(a), the curves obtained for different temperatures converge into one common line, at high applied fields. The barrier height for hole injection into the HOMO through the Al/P3HT interface can be, therefore, estimated as 0.85 eV. In Fig. 5(b), instead, the slopes are temperature dependent. The upper limit of the barrier height for hole injection into the HOMO through the ITO/P3HT interface is 0.47 eV at $T=100$ K. This indicates that the barrier height, defined as the energy gap between the HOMO of the polymer and the respective electrode work function, slightly varies with temperature in different ways. Note that the variation of band bending in the vicinity of contacts, if present, may be responsible for the latter. The deviation from straight line behavior at lower electric fields is attributed to thermionic emission. Therefore, the injection of holes through the lower barrier (ITO/P3HT) is expected to be more influenced by temperature.

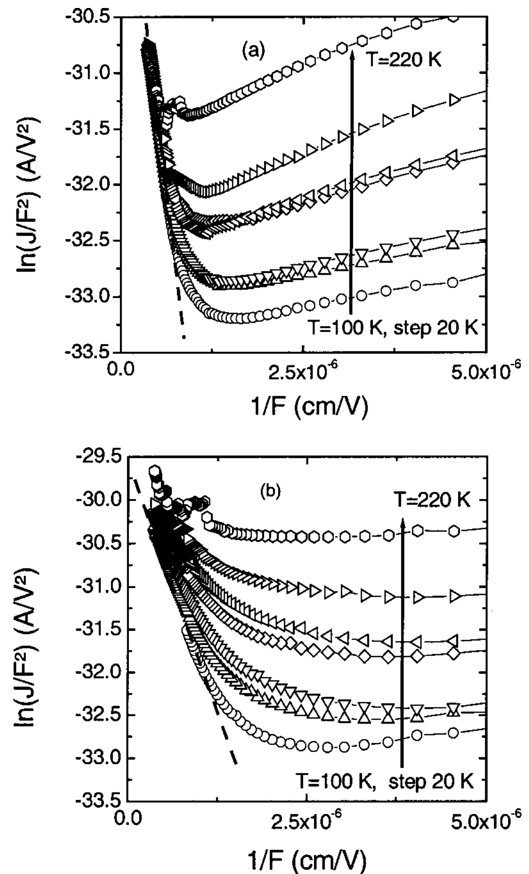

FIG. 5. Fowler–Nordheim plots for the tunneling of holes (a) from Al into P3HT and (b) from ITO into P3HT. Dotted lines indicate the linear parts of the curves.

We have also calculated the HOMO of the polymer using the procedure suggested by Hümmelgen *et al.*,[26] where knowledge of the thickness and the effective mass is not required, but only the work functions of electrode materials and the slopes of the FN curves in reverse and in forward bias, at constant temperature. In this procedure, the ratio of the slopes of the FN curves, from Eq. (9), is considered. Such calculations suggest a linear variation of the HOMO from about 5.24 eV at 100 K to about 4.9 eV at 220 K, if the electrode work functions were constant with temperature.

D. Transition from field to thermal emission limited characteristics

The concept of tunneling alone, or of thermionic emission alone, does not make much sense within the transition region. The description of this region would call for some kind of a hybrid model. The combined contribution of the two phenomena to the measured current has been described either as field assisted thermionic emission or thermally ac-

Downloaded 05 Aug 2003 to 134.106.114.81. Redistribution subject to AIP license or copyright, see http://ojps.aip.org/japo/japcr.jsp

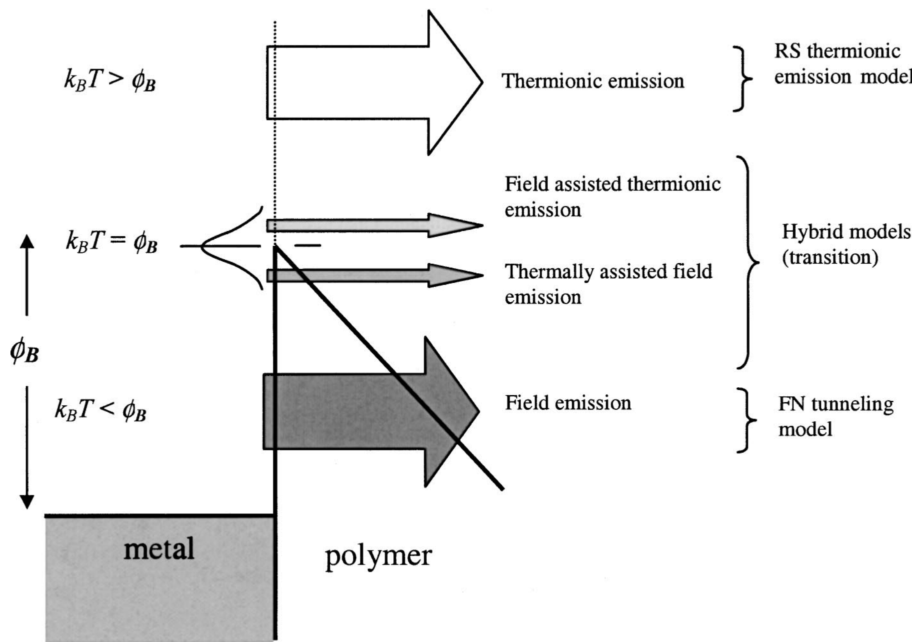

FIG. 6. Mechanisms of charge carrier injection through a metal/polymer interface. The energy distribution function is of Maxwell—Boltzmann type.

tivated tunneling[24] (see Fig. 6). The increase in electric field implies a stronger barrier lowering (due to image charge), meaning that charge carriers which have a smaller energy can now be emitted over the barrier, and this is denoted as field assisted thermionic emission. On the other hand, since the barrier is considered to be constant in the FN theory, an increase in temperature implies a smaller difference between the energies of the electrons and the top of the barrier, meaning that the barrier to be traversed is now thinner, and the probability of tunneling increases. This is denoted as thermally assisted field emission.

Indeed, many studies have been done in other metal/polymer/metal devices, in this respect. For instance, temperature dependent current-voltage measurements on poly-para-phenylene venylene (PPV) films revealed a thermally activated behavior at low voltages.[27] The absence of this behavior at higher voltages was attributed to field emission (FN tunneling) at the contacts.[28] However, the theoretical FN expression was not able to quantitatively account for their experimental J-V characteristics. The large deviations were attributed to thermionic emission,[29] space charge effects in the bulk of the polymer,[30] and band bending effects.[31] It has been demonstrated that at low electric fields and at room temperature the conduction of holes in PPV devices is limited by space charge effects in the bulk of the polymer and not by the charge injection from the contact.[32] At high fields, however, the strong field dependence of the current together with its decreased temperature dependence both seem to argue in favor of the tunneling model.[33]

The shortcomings of each of the models RS and FN considered separately, are the following: At high electric fields, barrier lowering may be comparable to the barrier height itself, and its neglect in tunneling considerations is problematic. Also problematic are the assumptions of a triangular barrier and the existence of a continuum of unbound states into which carriers can tunnel. The application of the RS concept suffers from the neglect of inelastic carrier scattering inside the potential well which is of crucial importance in organic solids where transport is an incoherent process and the mean free path is small. There, clearly, is a need for the harmonization of the two concepts, the classical RS thermionic emission over the barrier and the quantum mechanical FN tunneling through the barrier.

1. Model

We utilize the expression for the temperature dependent tunneling current through a triangular barrier at metal/polymer interfaces derived in,[14,22] from which we deduce an expression for the minimum electric field that must be applied to a device with a known interface barrier height, at a given temperature T, so that the tunneling contribution equals the thermionic emission contribution to the current. The tunneling current density through the triangular barrier at a metal polymer interface, considering the effect of temperature on the Fermi distribution is given by[14]

$$J(T)=\frac{q^2\pi k_BT}{h^2}\left(\frac{m^*}{2\phi_B}\right)^{1/2}F \times\exp\left(-\frac{8\pi\sqrt{2m^*}\phi_B^{3/2}}{3hqF}\right)\frac{1}{\sin(\beta\pi k_BT)}, \tag{12}$$

where

$$\beta=\frac{4\pi\sqrt{2m^*}\phi_B^{1/2}}{Fqh}. \tag{13}$$

Further, this expression is only applicable if the following condition is satisfied:

$$\beta<\frac{1}{k_BT}-\frac{1}{\phi_B}. \tag{14}$$

Substituting Eq. (13) in Eq. (14), we obtain an explicit relationship (15) between temperature, applied electric field, and

Downloaded 05 Aug 2003 to 134.106.114.81. Redistribution subject to AIP license or copyright, see http://ojps.aip.org/japo/japcr.jsp

interface barrier height, for the threshold field that must be applied, for tunneling to dominate the J-V characteristics

$$F>\frac{2\sqrt{2m}k_B T\phi_B^{3/2}}{q\hbar(\phi_B-k_B T)}. \tag{15}$$

The inequality (15) is not defined for $\phi_B=k_BT$, since this would mean that there is no barrier. This is logical considering that the definition of tunneling demands that the energy of the electrons must be smaller than the barrier height, otherwise, for $\phi_B<k_BT$, thermionic emission of electrons across the barrier occurs.

In the low-temperature limit, for temperatures such that $k_BT\ll\phi_B$, the denominator of inequality (15) may be considered as independent of T. However, as T is increased, k_BT approaches ϕ_B, and the required field becomes very high and then tends to infinity. For two different barriers $\phi_{B1}<\phi_{B2}$, it can occur, for example, that for ϕ_{B1} no more tunneling is possible, but for ϕ_{B2} it can still be observed.

The fact that there is no single valued energy for all electrons in a material, but rather distributed energy values about the average energy k_BT according to the Maxwell–Boltzmann statistics, indicates that a portion $\exp(-E/k_BT)$ of the electrons will have energies values larger than E. When this portion has crossed over the barrier, we cannot distinguish them from those that have tunneled. Another difficulty arises from the fact that there might be no single valued barrier height, but a distribution around ϕ_B, due to the fuzziness in the energy of the polymer band edges caused by disorder.[28] In addition, the evaporated electrodes are not expected to have precisely known values of the work function due to their amorphous structure. The above implies that analysis of either tunneling or thermionic emission makes real sense away from the transition region.

The inequality (15) has been evaluated for different interface barriers ϕ_B (in eV), where $m=9.11\times10^{-31}$ kg, $k_B=8.62\times10^{-5}$ eV/K, T is the absolute temperature, $q=1.60\times10^{-19}$ C, $h=6.64\times10^{-34}$ Js. The result of this evaluation for interface barriers ranging from 0.015 and 0.05 eV is shown in Fig. 7(a), which shows plots of the minimum electric field F_z which must be applied to a metal/semiconductor polymer/metal device, in order for charge carriers to be injected across the barrier through quantum mechanical tunneling, as a function of temperature.

At the field F_z tunneling balances thermionic emission, i.e., for any particular interface potential barrier ϕ_B, at a given temperature T, it is necessary to apply an electric field F_z so that the number of electrons injected from the metal into the semiconducting polymer through quantum mechanical tunneling becomes equal to that due to thermionic emission.

The vertical dotted line indicates the value of T such that $k_BT=\phi_{B1}$, i.e., the temperature at which the average energy of the charge carriers becomes equal to the potential barrier height. The region to the left of this line indicates the temperatures at which $k_BT<\phi_{B1}$. Charge carriers with such energies can only be injected into the semiconductor by quantum mechanical tunneling. The curve approaches the indicated vertical line asymptotically.

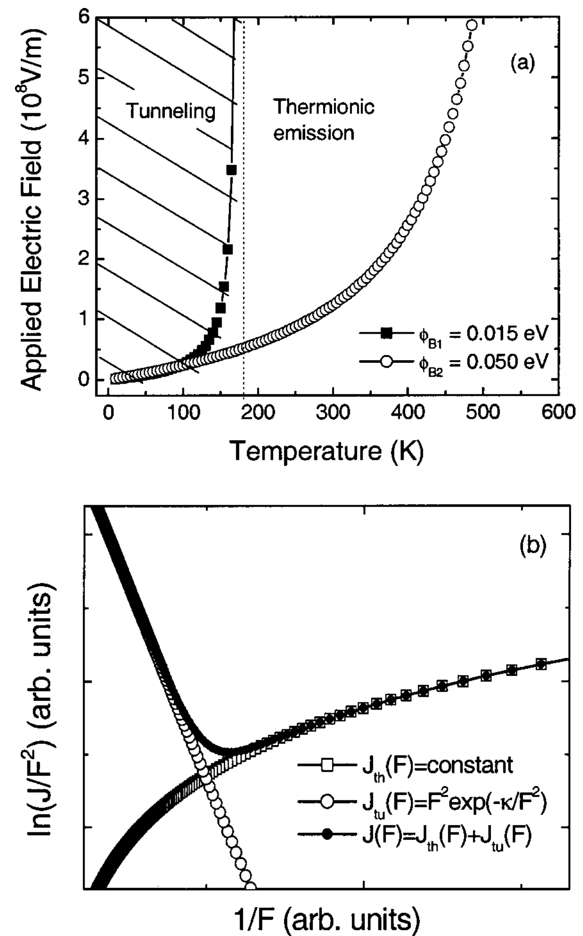

FIG. 7. (a) Theoretical curves [inequality (16)] showing the boundary between thermionic emission and field emission characteristics for different interface barriers, $\phi_{B1}=0.015$ eV; $\phi_{B2}=0.05$ eV. The shaded area corresponds to field and temperature combinations described by field emission (tunneling). Outside this area, thermionic emission describes the charge injection. The dotted line indicates the temperature at which $k_BT=\phi_{B1}$. (b) The superposition of contributions of thermionic $J_{th}(F)$ (open squares) and tunneling $J_{tu}(F)$ (open circles) in total current density $J(F)$ (closed circles). In the thermionic term, the potential barrier is considered as field-independent.

If the applied field is smaller than F_z, the injection is dominated by thermionic emission, otherwise it is dominated by tunneling, provided the temperature is well below the critical value determined by the condition $k_BT=\phi_B$. If T increases, a relatively higher field is required for tunneling to balance thermionic emission. If T is such that k_BT is smaller but comparable to ϕ_B, it becomes important to consider the distribution of energies of charge carriers about k_BT (as mentioned above), and the thermionic emission will dominate. As k_BT approaches to ϕ_B, the electric field F_z tends to infinity, therefore, the definition of tunneling ceases to make sense.

The above can be summarized as follows: For an interface barrier ϕ_B, any combination of $F>F_z$ and T such that $k_BT<\phi_B$, tunneling dominates the injection at the electrode/metal interface (shaded region). Outside this region, thermionic emission dominates. Below and on the right hand side of the F_z curve, the J-V characteristics should be indepen-

Downloaded 05 Aug 2003 to 134.106.114.81. Redistribution subject to AIP license or copyright, see http://ojps.aip.org/japo/japcr.jsp

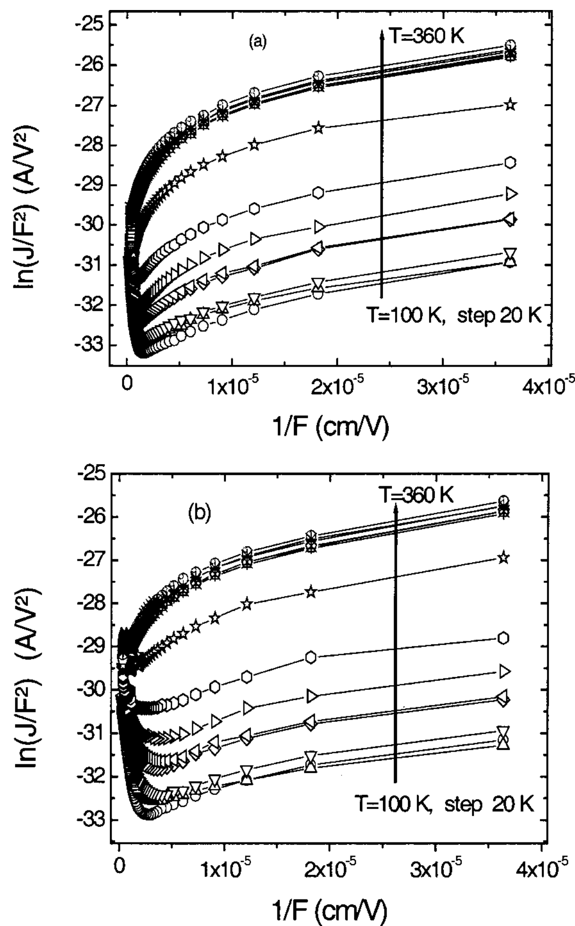

FIG. 8. Fowler–Nordheim plots for the tunneling of holes (a) from Al into P3HT and (b) from ITO into P3HT for an ITO/P3HT/Al device in the temperature range 100–360 K.

dent of tunneling, and the rate of change of the current with applied field is reduced. We should, therefore, expect the bulk properties of the polymer to take over the current limitation, since the electrons do not "see" a barrier. Depending on the mobility of the electrons in the polymer, either ohmic behavior or space charge limitation will be observed.

2. Comparison with experiment

It has frequently been indicated that the deviation of the FN plot from straight lines at low electrical fields might be due to the contribution of thermionic emission, so most authors truncate their FN curves when the slight curvature starts to appear,[14,26,28,34] in order to analyze only the straight line regime, estimate the slope and, hence, the barrier height. In Fig. 8, we show complete FN curves obtained for our devices under (a) forward and (b) reverse bias, in the temperature range 100 to 360 K. Similar shape of curves was obtained also by Kiy *et al.*[35] for electron tunneling from a magnesium contact into Alq_3. As discussed in Sec. III C, the slopes are different, yielding a larger barrier for the hole injection through the Al/P3HT interface. The complete plot indicates a straight line at high field strength, which curves, reaches a minimum, and then gradually increases for lower applied fields. The contribution of field emission decreases, and the contribution from thermionic emission becomes ap-

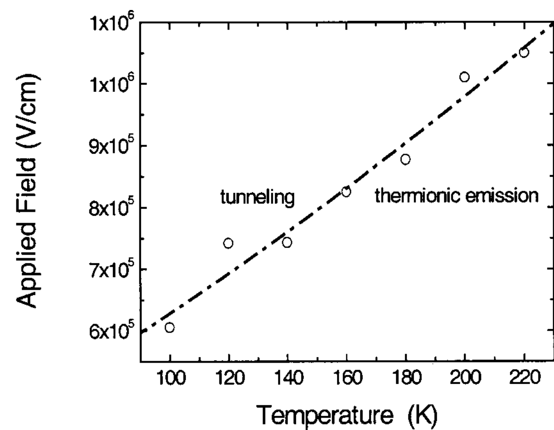

FIG. 9. Field at minima of Fowler–Nordheim plots as a function of temperature for ITO/P3HT/Al under reverse bias. The dashed line is a guide for the eye.

preciable and dominates the J-V characteristics thereafter. The overall behavior is schematically represented in Fig. 7(b), where the superposition of contributions of both effects, thermionic $J_{th}(F)$ and tunneling $J_{tu}(F)$, results in a minimum. Note that in the thermionic term the potential barrier is considered as field-independent.

At low temperatures, a relatively low electric field strength is required, in order to inject an appreciable number of holes by tunneling, for their density to become comparable to that of those that are injected thermionically. The minimum of the FN plot will shift towards higher applied field strength [to the left in Figs. 5, 7(b), and 8(a)] with an increase in temperature. The electric field at which the minimum of the FN curves is observed has been obtained from Fig. 5(a) and plotted against temperature, as shown in Fig. 9. The trend conforms to inequality (15).

If the temperature is high enough, the tunneling regime will not be seen in the FN plot [see Fig. 8(a), $T>260$ K]. The J-V behavior becomes nearly temperature independent. As T increases beyond $k_B T=\phi_B$, the J-V curves become bunched together (see Fig. 3).

We may conclude that for any description of the J-V characteristics as contact limited, or bulk limited, it is essential to specify the interface potential barrier, temperature, and applied electric field ranges where such limitation would be valid.

IV. CONCLUSIONS

We have shown that the current in ITO/P3HT/Al devices is limited by hole injection at the Al/P3HT contact when the device is reverse biased. The current becomes space charge limited at high voltages when tunneling contributes significantly to the charge injection. The electric field at which the transition from contact limited to space charge limited current takes place increases with temperature. If the current through the device is contact limited, the field of transition from thermionic emission to field emission increases with temperature, tending to infinity when the charge carrier energy is comparable to the interface barrier height. In forward bias, the ITO/P3HT interface supplies a high amount of

Downloaded 05 Aug 2003 to 134.106.114.81. Redistribution subject to AIP license or copyright, see http://ojps.aip.org/japo/japcr.jsp

charge in the polymer semiconductor bulk, and the current is space charge limited in the whole voltage and temperature range studied, suggesting the formation of an ohmic contact for hole injection at the ITO/P3HT interface. In the temperature range 100–220 K, we may estimate the hole injection barrier heights for Al/P3HT and ITO/P3HT as 0.85 and 0.47 eV, respectively.

ACKNOWLEDGMENTS

The authors acknowledge the Geselschaft für Technische Zusamenarbeit (GTZ), the Deutscher Academischer Austauschdienst (DAAD), and the German Ministry for Education and Research (BMBF) (Projects 01SF0026, 01SF0119) for funding their work. Many thanks go to the following persons for their contribution in various discussions and technical assistance: C. Deibel, E. von Hauff, D. Chirvase, V. Mertens, I. Riedel, M. Pientka, A. Geisler, and H. Koch.

[1] H. S. Nalwa, *Handbook of Advanced Electronic and Photonic Materials and Devices* (Academic Press, New York, 1997).
[2] H. S. Nalwa, *Handbook of Organic Conductive Molecules and Polymers* (Wiley, Canada, 1997).
[3] T. A. Skotheim, R. L. Elsenbaumer, and J. Ronalds, *Handbook of Conducting Polymers* (Marcel Dekker, New York, 1998).
[4] J. C. Scott, S. Karg, and S. A. Carter, J. Appl. Phys. **82(3)**, 1454 (1997).
[5] H. S. Nalwa, *Handbook of Surfaces and Interfaces of Materials* (Academic Press, New York, 2001).
[6] W. Brütting, S. Berleb, and A. Mückl, Organic Electronics **2**, 1 (2001).
[7] I. D. Parker, Y. Cao, and C. Y. Yang, J. Appl. Phys. **85**, 2441 (1999).
[8] D. V. Khramtchenkov, H. Bässler, and V. I. Arkhipov, J. Appl. Phys. **79**, 9283 (1996).
[9] D. Chirvase, Z. Chiguvare, M. Knipper, J. Parisi, V. Dyakonov, and J. C. Hummelen, J. Appl. Phys. **93**, 3376 (2003).
[10] V. Dyakonov, Physica E (Amsterdam) **14**, 53 (2002).
[11] H. E. Katz, A. Dodabalapur, Z. Bao, *Handbook of Oligo- and Polythiophenes*, edited by D. Fichou (Wiley-VCH, Weinheim, 1998).
[12] C. D. Dimitakopoulos and D. J. Mascaro, Organic Electronics **45**, 11 (2001).
[13] S. M. Sze, *Semiconductor Devices* (Wiley, New York, 1981).
[14] M. Koehler and I. A. Hümmelgen, Appl. Phys. Lett. **70**, 3254 (1997).
[15] A. J. Campbell, D. D. C. Bradley, and D. G. Lidzey, J. Appl. Phys. **82**, 6326 (1997).
[16] M. A. Lampert and P. Mark, *Current Injection into Solids* (Academic Press, New York, 1970).
[17] M. Abkowitz, J. S. Facci, and J. Rehm, J. Appl. Phys. **83**, 2670 (1998).
[18] M. Abkowitz, J. S. Facci, and M. Stolka, Appl. Phys. Lett. **63**, 1892 (1993).
[19] D. Chirvase, Z. Chiguvare, M. Knipper, J. Parisi, V. Dyakonov, and J. C. Hummelen, Synth. Met. **1**, 10 348 (2003).
[20] R. Valaski, L. M. Moreira, L. Micaroni, and I. A. Hümmelgen, J. Appl. Phys. **92**, 2035 (2002).
[21] M. Onoda, K. Tada, A. A. Zakhidov, and K. Yoshino, Thin Solid Films **331**, 76 (1998).
[22] K. C. Kao and W. Hwang, *Electrical Transport in Solids, with Particular Reference to Organic Semiconductors*, International Series in the Science of the Solid State, Vol. 14 (Pergamon Press, Oxford, 1981).
[23] Rasmi R. Das, P. Battacharya, W. Perez, Ram S. Katiyar, and A. S. Bhalla, Appl. Phys. Lett. **81**, 880 (2002).
[24] H. K. Henisch, *Semiconductor Contacts, An approach to ideas and models*, International Series of Monographs on Physics No. 70 (Clarendon Press, Oxford, 1984).
[25] P. S. Davids, Sh. M. Kogan, I. D. Parker, and D. L. Smith, Appl. Phys. Lett. **71**, 930 (1997).
[26] I. A. Hümmelgen, S. Roman, F. C. Nart, L. O. Peres, and E. L. de Sa, Appl. Phys. Lett. **68**, 3194 (1996).
[27] R. N. Marks, D. D. C. Bradley, R. W. Jackson, P. L. Burn, and A. Holmes, Synth. Met. **57**, 4128 (1993).
[28] I. D. Parker, J. Appl. Phys. **75**, 1656 (1994).
[29] H. Vestweber, J. Pommerrehne, R. Sander, R. F. Mahrt, A. Greiner, W. Heity, and H. Bässler, Synth. Met. **68**, 263 (1995).
[30] P. E. Burrows and S. R. Forrest, Appl. Phys. Lett. **64**, 2285 (1994).
[31] E. Ettedgui, H. Rayafitrimo, Y. Gao, and B. R. Hsieh, Appl. Phys. Lett. **67**, 2705 (1995).
[32] P. W. M. Blom, M. J. M. de Jong, and J. J. M. Vleggaar, Appl. Phys. Lett. **68**, 3308 (1996).
[33] P. W. M. Blom, M. J. M. de Jong, and M. G. van Munster, Phys. Rev. B **55**, R656 (1997).
[34] J. R. de Lima, C. Schreiner, I. A. Hümmelgen, C. C. M. Fornari, Jr., C. A. Ferreira, and F. C. Nart, J. Appl. Phys. **84**, 1445 (1998).
[35] M. Kiy, I. Biaggio, M. Koehler, and P. Günter, Appl. Phys. Lett. **80**, 4366 (2002).

Downloaded 05 Aug 2003 to 134.106.114.81. Redistribution subject to AIP license or copyright, see http://ojps.aip.org/japo/japcr.jsp